



Aberrant posterior cingulate connectivity classify first-episode schizophrenia from controls: A machine learning study

Sugai Liang^{a,b}, Wei Deng^{a,b}, Xiaojing Li^a, Qiang Wang^a, Andrew J. Greenshaw^c, Wanjun Guo^{a,b}, Xiangzhen Kong^d, Mingli Li^a, Liansheng Zhao^a, Yajing Meng^a, Chengcheng Zhang^a, Hua Yu^a, Xin-min Li^c, Xiaohong Ma^a, Tao Li^{a,b,*}

^a Mental Health Center, Psychiatric Laboratory, State Key Laboratory of Biotherapy, West China Hospital, Sichuan University, Chengdu 610041, Sichuan, China

^b West China Brain Research Centre, West China Hospital, Sichuan University, Chengdu 610041, Sichuan, China

^c Department of Psychiatry, University of Alberta, Edmonton T6G 2B7, AB, Canada

^d Language and Genetics Department, Max Planck Institute for Psycholinguistics, Nijmegen 6525, XD, Netherlands

ARTICLE INFO

Article history:

Received 15 November 2019

Received in revised form 23 February 2020

Accepted 10 March 2020

Available online 24 March 2020

Keywords:

Schizophrenia
Posterior cingulate cortex
Default mode network
Classification
Gradient boosting

ABSTRACT

Background: Posterior cingulate cortex (PCC) is a key aspect of the default mode network (DMN). Aberrant PCC functional connectivity (FC) is implicated in schizophrenia, but the potential for PCC related changes as biological classifier of schizophrenia has not yet been evaluated.

Methods: We conducted a data-driven approach using resting-state functional MRI data to explore differences in PCC-based region- and voxel-wise FC patterns, to distinguish between patients with first-episode schizophrenia (FES) and demographically matched healthy controls (HC). Discriminative PCC FCs were selected via false discovery rate estimation. A gradient boosting classifier was trained and validated based on 100 FES vs. 93 HC. Subsequently, classification models were tested in an independent dataset of 87 FES patients and 80 HC using resting-state data acquired on a different MRI scanner.

Results: Patients with FES had reduced connectivity between PCC and frontal areas, left parahippocampal regions, left anterior cingulate cortex, and right inferior parietal lobule, but hyperconnectivity with left lateral temporal regions. Predictive voxel-wise clusters were similar to region-wise selected brain areas functionally connected with PCC in relation to discriminating FES from HC subject categories. Region-wise analysis of FCs yielded a relatively high predictive level for schizophrenia, with an average accuracy of 72.28% in the independent samples, while selected voxel-wise connectivity yielded an accuracy of 68.72%.

Conclusion: FES exhibited a pattern of both increased and decreased PCC-based connectivity, but was related to predominant hypoconnectivity between PCC and brain areas associated with DMN, that may be a useful differential feature revealing underpinnings of neuropathophysiology for schizophrenia.

© 2020 The Authors. Published by Elsevier B.V. This is an open access article under the CC BY-NC-ND license (<http://creativecommons.org/licenses/by-nc-nd/4.0/>).

1. Introduction

Schizophrenia is a severe and complex psychiatric disorder associated with aberrant brain functional connectivity (FC). Prior neuroimaging studies have demonstrated schizophrenia has abnormal connectivity in the default mode network (DMN), which is the most frequently studied network in resting-state functional magnetic resonance imaging (rs-fMRI) (Bluhm et al., 2007; Ebisch et al., 2018; Garrity et al., 2007; Rotarska-Jagiela et al., 2010). The posterior cingulate cortex (PCC) is a crucial component of DMN, which plays a central role in gathering information, retrieving episodic memory, supporting internally-directed

cognition, and regulating the focus of attention (Fransson and Marrelec, 2008; Greicius et al., 2003; Leech and Sharp, 2014; Raichle et al., 2001). Patients with schizophrenia had altered connectivity between the PCC and other brain regions associated with the DMN (Bluhm et al., 2007; Rotarska-Jagiela et al., 2010; Whitfield-Gabrieli et al., 2009). The anomalous connectivity of PCC could be associated either with predisposition to, or a greater risk for schizophrenia (Whitfield-Gabrieli et al., 2009). Additionally, both positive and negative symptoms in schizophrenia contributed to modulate the altered connectivity with the PCC (Bluhm et al., 2007; Garrity et al., 2007; Rotarska-Jagiela et al., 2010; Zhou et al., 2008). Furthermore, the reduced gray matter volume of PCC could be linked with poor outcome of schizophrenia (Mitelman et al., 2005). The abnormal glucose metabolism in PCC and microstructure anomalies of cingulum were also revealed in patients with schizophrenia (Haznedar et al., 2004; Leech and Sharp, 2014; Samartzis et al., 2014). In fact,

* Corresponding author at: West China Mental Health Centre, West China Hospital, Sichuan University, No. 28th Dianxin Nan Str., Chengdu, Sichuan 610041, China.
E-mail address: xuntao26@hotmail.com (T. Li).

there is limited direct evidence available to indicate whether the aberrant PCC connectivity may be a useful biomarker to predict schizophrenia.

The dysconnectivity of brain networks in schizophrenia underlying rs-fMRI has been identified in seed-based analysis studies (Yu et al., 2012). Using the PCC as a region-of-interest (ROI) brain area, in patients with schizophrenia, hypoconnectivity between the seed and the lateral parietal, medial prefrontal, and cerebellar regions have been observed (Bluhm et al., 2007; Rotarska-Jagiela et al., 2010). Increased FCs also have been reported in the PCC and the frontal lobe in patients diagnosed with schizophrenia (Venkataraman et al., 2012; Whitfield-Gabrieli et al., 2009). The divergent findings of prior research may be due to a number of factors including differences in data preprocessing, statistical approaches, and biological and clinical heterogeneity of features of symptomatology in schizophrenia (Liang et al., 2019). Further analysis of large independent samples is necessary to confirm which specific brain regions and their FCs contribute most to schizophrenia.

Considering the computational load of appropriate analysis in this context, quite often the input feature dimensionality is restricted in the attempt to examine voxel-wise connectivity studies (Meng et al., 2016). Applying a high-dimensional voxel-based brain-wide strategy combined with region-based analysis to further verify the results, may provide both greater confidence and accuracy in identifying aberrant connectivity patterns of schizophrenia (Cheng et al., 2015). Hence, we proposed to use via machine learning analysis of PCC-based/brain-wide voxel-wise searching combined with regional FCs.

We attempted to conduct a brain-wide seed-based approach in rs-fMRI data to discover PCC-based region- and voxel-wise FCs to distinguish patients with first-episode schizophrenia (FES) from healthy control individuals (HC). We replicated our key findings in terms of neurobiological distinction in an independent “holdout” cohort, to provide most robust evidence for alterations of brain functional connectivity in schizophrenia.

2. Materials and methods

2.1. Participants

A total of 360 right-handed Chinese subjects (187 FES patients and 173 HC) participated in this study. All subjects provided informed consent in accord with requirement of the ethics committee of the West China Hospital of Sichuan University. Dataset 1 including 100 patients with FES (mean age 24.50 years, 49 females) and 93 controls (mean age 24.68 years, 58 females), was used to identify the highest degree of discriminative functional connectivity and train classification model to predict FES patients. Dataset 2 including 87 patients with FES (mean age 24.91 years, 49 females) and 80 controls (mean age 26.13 years, 41 females), was applied to validate the classification models. Dataset 1 was acquired with 3.0 Tesla (T) Philip MRI machine, and Dataset 2 with 3.0 T GE MRI machine. In each dataset, age and sex were demographically matched for patients with FES and HC. Subject demographics are displayed in Tables S1 & S2. Symptom severity was evaluated using the Positive and Negative Scale (PANSS). Further subject details are provided in Supplementary material.

2.2. Image acquisition

Resting-state fMRI and high-resolution T1-weighted imaging data were acquired from each participant. All subjects were instructed to rest and keep awake (eyes closed) during scanning, and monitored via a video camera in the scanner console room. See detailed scanning parameters in Supplementary material.

2.3. Data preprocessing

All datasets were preprocessed using FSL tools (www.fmrib.ox.ac.uk/fsl) (Smith et al., 2004). fMRI volumes were registered to the individual's structural scans and standard space images using FMRIB's Linear Image Registration Tool (FLIRT) (Jenkinson et al., 2002). Here, temporal bandpass filtering (0.01–0.08 Hz) was used to reduce the effect of low frequency drift and high frequency physiological noise. Nuisance signal (6 motion parameters, white matter, cerebrospinal fluid, and global signal for each individual) were eliminated using linear regression. Subjects with framewise displacement >0.3 mm were excluded from all further analysis steps (Power et al., 2012). After quality control, dataset 1 had 93 patients and 90 controls left and no subjects were excluded in the dataset 2.

Considering findings reported that global signal variability may be elevated, especially in patients with schizophrenia (Gotts et al., 2013; Yang et al., 2014), we examined separately results without implementing global signal regression (GSR); all other analysis remained unchanged.

2.4. Seed-based region-wise analysis

For each participant's rs-fMRI data, seed-based correlation approach was used to extract the time course from the PCC. The seed was constructed by forming a 10-mm sphere centered at foci as defined by MNI space (0, –53, 26) (Andrews-Hanna et al., 2007; Van Dijk et al., 2010). Then, for each subject, we computed the Pearson correlation coefficient between time course from the PCC and the time course from 90 brain regions identified in the automated anatomical labeling (AAL) atlas. Temporal correlation coefficients relative to the PCC were converted to z-scores using Fisher's r-to-z transformation. Multiple linear regression was conducted to control for age and sex related effects on FCs.

2.5. Brain-wide seed-based voxel-wise analysis

Based on the AAL atlas, each rs-fMRI image included 47,636 voxels (Cheng et al., 2015). Seed-to-voxel FCs were calculated as the correlation coefficient between time courses from the PCC and the time courses from all voxels using temporal correlation followed by Fisher z-transformation for each subject. Effect of age and sex were regressed out for each dataset at this step.

2.6. Machine learning analysis

All analyses were computed based on scikit-learn (Pedregosa et al., 2011) and Nilearn (<https://nilearn.github.io/index.html>). Fig. 1 illustrates the main steps in data analysis pipeline.

2.6.1. Feature selection

SelectFdr (*f_classif*) of scikit-learn was applied to identify significant FCs to differentiate patients with FES from HC with FDR correction (false discovery rate, $P_{corrected} < 0.05$). In region-wise analysis, the most discriminative features were selected from FCs between the PCC and ninety regions defined in the AAL atlas. We also studied the association between the selected FCs and severity of clinical symptoms. In voxel-wise analysis, the most differential features were selected from FCs between the PCC and all 47,636 voxels. Considering the selected voxels were distributed sparsely across the brain, we employed a “26-connected neighborhood” strategy as the connectivity criterion (Bazin et al., 2011; Meng et al., 2016). BrainNet Viewer was used to visualize the seed-based FCs (Xia et al., 2013).

2.6.2. Classification analysis

We implemented the Gradient Boosting Decision Tree (GBDT) - an ensemble machine learning algorithm to distinguish patients with FES from HC. GBDT is an improved boosting algorithm for classification

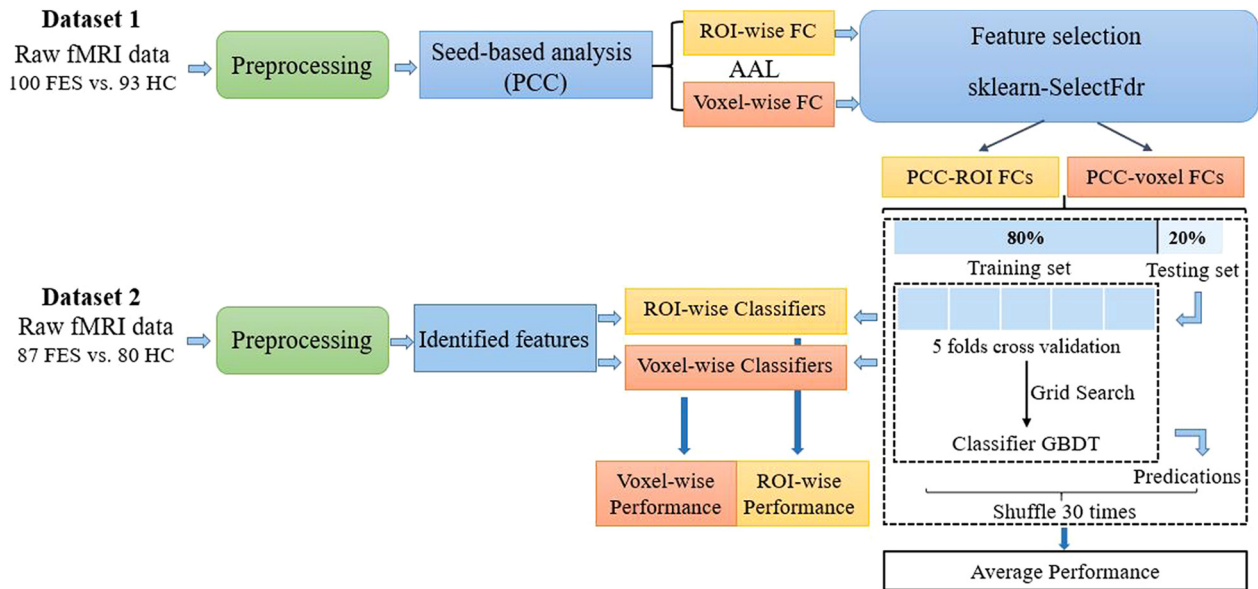


Fig. 1. Data analysis flowchart. PCC, posterior cingulate cortex. GBDT, gradient boosting decision tree. FC, functional connectivity. ROI, region-of-interest. AAL, automated anatomical labeling atlas. FDR, false discovery rate.

problems (Friedman, 2001). With high flexibility and robust in multivariate application, GBDT has been widely used in classification and prediction of psychiatric disorders (Chekroud et al., 2016; Liang et al., 2019; Natekin and Knoll, 2013).

2.6.2.1. Training and testing classification models in Dataset 1. Dataset 1 was shuffled 30 times to avoid any element of bias/patterns in the split datasets. After each shuffle, Dataset 1, with the selected features (region- and voxel-wise FCs), were separated into training model set (80%) and testing set (20%). In training model set, grid search with 5-fold cross-validation was employed to determine the optimal parameters. The procedure was repeated 30 times, and obtained 30 classifier models. Then testing set were fed into the trained classifiers and thus obtained the averaged performance including mean accuracy, sensitivity, specificity, positive and negative predictive values, and the area under the receiver operating characteristic curve (AUC).

2.6.2.2. Testing classification models in Dataset 2. We tested classifiers in an independent replication data set (Dataset 2). The identified PCC-based region-/voxel-wise FCs were extracted from Dataset 2. Then the selected features were fed into the trained models to classify FES patients from HC. As described above, to reflect model performance objectively and conservatively, average classification measures were computed for the independent cohort. More details on the classification procedure are described in Supplementary material.

3. Results

3.1. PCC-based region-wise connectivity

In region-wise analysis, FCs between the PCC and twenty-one brain regions were identified as the most distinctive features to distinguish patients with FES from HC in Dataset 1. Fig. 2 illustrates the seed-based region-wise FCs. The details of brain areas are listed in the Table S3. Compared to HC, patients with FES had decreased FCs between the PCC and the bilateral supplementary motor area (SMA), the bilateral precuneus (PCUN), right middle frontal gyrus (MFG), right opercular part of inferior frontal gyrus (IFGoperc), right triangular part of inferior frontal gyrus (IFGtriang), right orbital part of inferior frontal gyrus (ORBinf), right insula (INS), right inferior parietal lobule (IPL), left orbital part of middle frontal gyrus (ORBmid), left parahippocampal

gyrus (PHG), and left anterior cingulate cortex and paracingulate gyri (ACG). Patients with FES had increased FCs between the PCC, and the left inferior temporal gyrus (ITG), and left olfactory cortex (OLF).

In patients with FES, FCs between the PCC and the right IFGoperc was correlated with the positive and negative symptoms ($r = -0.29$, $P_{uncorr} = 0.003$; $r = -0.28$, $P_{uncorr} = 0.004$). And connectivity between the seed and the right IFGtriang was associated with the positive and negative symptoms ($r = -0.27$, $P_{uncorr} = 0.02$; $r = -0.24$, $P_{uncorr} = 0.02$). Estimated with the selected FCs, an accuracy of 70.17% and an AUC of 70.07% were achieved in Dataset 1. The results of this study yielded an accuracy of 72.28% and an AUC of 72.77%, on the basis of the region-wise FCs in Dataset 2.

3.2. PCC-based voxel-wise connectivity

In voxel-wise analysis, FCs between the PCC and 2157 voxels were selected as the most distinctive features to classify patients with FES from HC in Dataset 1. Fig. 3, Figs. S1 and S2 illustrate the brain-wide voxel-wise selected clusters. Patients with FES relative to HC had hypoconnectivity between the PCC and the bilateral ACG, right IFGoperc, right IFGtriang, right ORBinf, right MFG, right SMA, right IPL, right PCUN, and left PHG at the voxel-wise level. Patients with FES had hyperconnectivity between the PCC, and the left ITG, and left middle temporal gyrus (MTG). Voxel-wise clusters differentiating patients from HC largely overlapped with region-wise selected brain areas that were functionally connected with PCC.

Using the seed-based voxel-wise FCs, an accuracy of 73.42% and an AUC of 73.41% were achieved in Dataset 1. The results of this study yielded an accuracy of 68.72% and an AUC of 69.07% using the selected voxel-wise FCs in Dataset 2.

Fig. S3 displays the comparison of classification accuracy of region- and voxel-wise FCs based on Dataset 1 and on Dataset 2. Averages and standard deviations of the classification performance measures are presented in the Supplementary Table S4 for these two datasets. Using seed-based voxel-wise FCs, classification accuracy was lower in Dataset 2, which was probably due to the high dimensionality of the data. The classification model based on the region-wise FCs achieved a more robust and relatively higher accuracy in Dataset 2.

As described earlier, considering the effects of global signal on the identified patterns, the significant features were also selected from Dataset 1 without GSR. The results based on the data without GSR

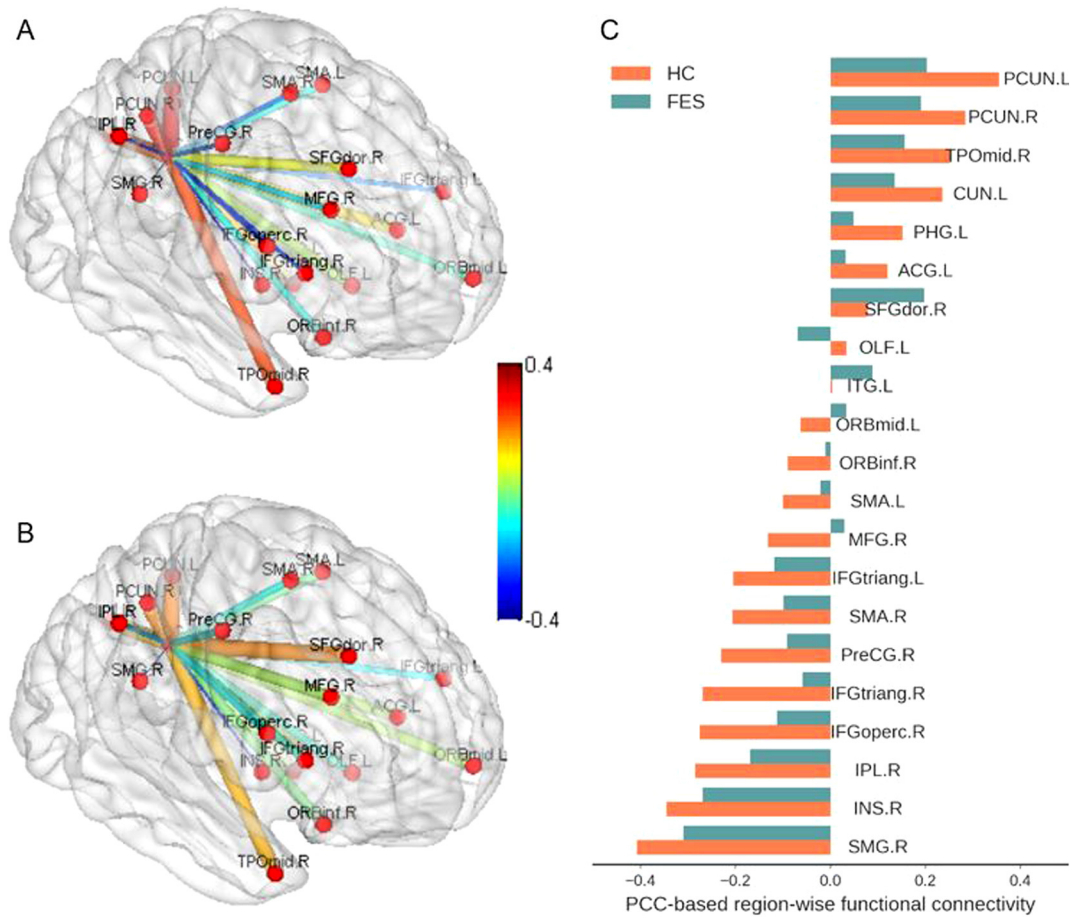


Fig. 2. Differential PCC-based region-wise functional connectivity for FES and HC. A HC, healthy controls. B FES, patients with first-episode schizophrenia. C comparisons between HC and FES in selected twenty-one PCC-based region-wise functional connectivity. Red dots represent selected brain areas functionally connected with PCC. L, left. R, right. PreCG, precentral gyrus. SFGdor, dorsolateral superior frontal gyrus. MFG, middle frontal gyrus. ORBmid, orbital part of middle frontal gyrus. IFGoperc, opercular part of inferior frontal gyrus. IFGtriang, triangular part of inferior frontal gyrus. SMA, supplementary motor area. OLF, olfactory cortex. INS, insula. ACG, anterior cingulate and paracingulate gyri. PHG, parahippocampal gyrus. CUN, cuneus. IPL, inferior parietal lobule. SMG, supramarginal gyrus. PCUN, precuneus. TPOmid, temporal pole of middle temporal gyrus. ITG, inferior temporal gyrus.

yielded accuracies of 70.26% and 73.85% for PCC-based region- and voxel-wise FCs, respectively. Independent two-sample *t*-test was conducted to compare the classification accuracies based on Dataset 1 with and without GSR (see Fig. S4). No significant statistical differences were found in classification accuracies neither in region-wise FCs ($T = -0.51$, $P_{uncorr} = 0.96$) or in voxel-wise FCs ($T = -0.20$, $P_{uncorr} = 0.84$) between Dataset 1 with and without GSR.

4. Discussion

In the current study, we applied a data-driven approach with the PCC-based region- and voxel-wise FCs to investigate abnormal brain patterns in patients with FES. Voxel-wise clusters corresponded well to region-wise selected brain areas which were functionally connected with the PCC that differentiated the category of patients with FES from HC. These brain areas included ACG, PHG, PCUN, IFGoperc, IFGtriang, MFG, ITG, SMA, and IPL. Notably, the PCC-based region-wise connectivity revealed a relatively high discriminatory ability in classifying individuals with FES from HC, with average accuracy as 72.28% in the independent sample set. In addition to the findings above, one of most important strength of our current study is that patients with FES exhibited concurrent increases and decreases in PCC-based connectivity abnormalities, but mostly reduced connectivity between the PCC and brain areas associated with the DMN.

A prior study using brain-wide PCC-based FC maps combined with support vector machine, achieved an accuracy of 55.6% to distinguish

patients with FES from HC (Mikolas et al., 2016). Additionally, in a previous study based on the AAL atlas with linear discriminant analysis, patients with schizophrenia relative to healthy comparisons exhibited predominately weaker inter-regional connectivity pattern, which could be used to predict the disorder with an accuracy of 76.34% (Li et al., 2019). In this study, we adopted an ensemble learning method – GBDT as classifier to two relatively large and independent sample sets of patients with FES (the majority were treatment-naïve). Classification accuracy based on differential region-wise FCs was moderate but more robust, confirmed in an independent cohort in our subsequent analysis. The classification performance of the current study based on resting-state FC was very similar to our prior findings of structural and diffusion tensor imaging study (Liang et al., 2019).

Most previous rs-fMRI studies have attempted to remove brain global signal to better isolate functional networks (Ciric et al., 2017; Lin et al., 2016). Related evidence has concerned that global signal may affect the findings in group-level comparisons between patients with psychiatric disorders and healthy individuals (Gotts et al., 2013; Yang et al., 2014). It is unclear whether global signal might influence the performance to distinguish patients with FES from HC. The present study attempted to rule out confounding factors of chronicity of the illness and treatment effects, and examined possible effects of brain global signal. Findings of this study suggested that global signal might not impact on the accuracy to discriminate patients with FES from HC at the individual level.

In the present study, patients with FES had reduced connectivity between the PCC and the frontal areas, ACG, PHG, and IPL, which were

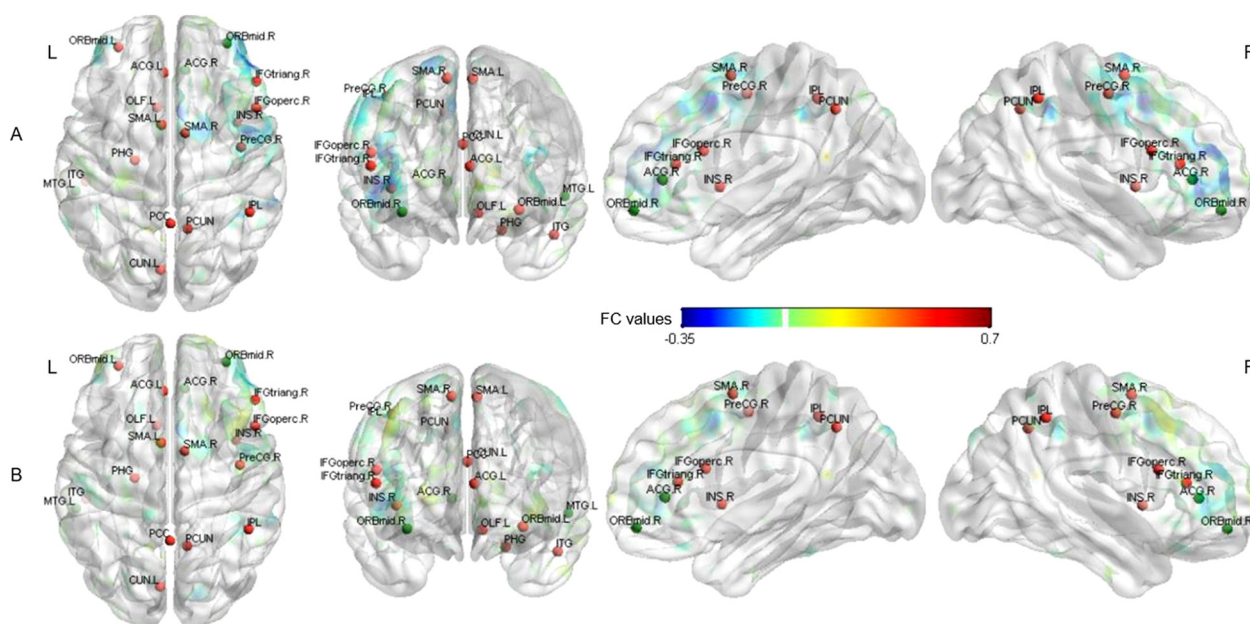


Fig. 3. Differential PCC-based voxel-wise functional connectivity for FES and HC. A HC, healthy controls. B FES, patients with first-episode schizophrenia. Red dots are voxel-wise clusters overlapped with the selected region-wise brain areas functionally connected with PCC. Green dots are clusters identified in voxel-wise analysis. L, left. R, right. ORBmid, orbital part of middle frontal gyrus. ACG, anterior cingulate and paracingulate gyri. MTG, middle temporal gyrus.

consistent with the findings of prior neuroimaging studies (Bluhm et al., 2007; Gao et al., 2018; Garrity et al., 2007; Rotarska-Jagiela et al., 2010; Zhang et al., 2018). This study also indicated that the abnormal FCs between the PCC and the inferior frontal areas were correlated with the severity of positive and negative symptoms in patients with schizophrenia. Similar findings have been reported in the previous research (Bluhm et al., 2007; Garrity et al., 2007). Prior studies showed that patients with schizophrenia had abnormal glucose metabolism, reduced gray matter volume, and white matter microstructure anomalies in the PCC (Haznedar et al., 2004; Leech and Sharp, 2014; Mitelman et al., 2005; Samartzis et al., 2014). Additionally, a post-mortem autoradiography study revealed that patients with schizophrenia had increased cannabinoid receptors (CB1) in the PCC (Newell et al., 2006). The CB1 receptor in positron emission tomography neuroimaging showed that binding levels (distribution volume) in the PCC were associated with the increased severity of positive symptoms in schizophrenia (Wong et al., 2010). Furthermore, hypoactivation within the PCC significantly was correlated with the positive symptoms induced by ketamine, which suggested that *N*-methyl-D-aspartate (NMDA) receptor hypofunction in the PCC was related to the pathophysiology of schizophrenia (Northoff et al., 2005). Combined with findings in this study, the structural and functional alterations of PCC may represent part of the neuronal basis of schizophrenia.

Brain regions identified as parts of DMN include PCC, PCUN, medial prefrontal gyrus, lateral temporal cortex, ACG, PHG, and IPL (Greicius et al., 2003; Raichle et al., 2001). DMN is involved in self-referential processing, social cognition and autobiographical memory retrieval, memory consolidation, monitoring one's own internal state and emotions (Buckner et al., 2008; Ebisch et al., 2018; Fransson and Marrelec, 2008; Leech and Sharp, 2014; Spreng et al., 2009). As known, PCC plays a pivotal role in DMN (Fransson and Marrelec, 2008; Leech and Sharp, 2014). The disrupted connectivity between the PCC and other brain areas of DMN was related to the long-term clinical outcome of patients with schizophrenia (Du et al., 2016; Lee et al., 2019). Polymorphism in schizophrenia risk gene *microRNA-137* was associated with the reduced functional and structural connectivity between the PCC and the anterior cingulate cortex and its adjacent prefrontal cortex in healthy controls, which could be a key aspect of brain mechanisms

linked to the underlying genetics of the disorder (Zhang et al., 2018). In the current study, patients with FES exhibited a pattern of both increased and decreased PCC-based connectivity, as hypoconnectivity between the PCC and the frontal areas, ACG, PHG, and IPL, and hyperconnectivity with respect to the lateral temporal regions. The present study manifested that patients with FES were related to the predominant hypoconnectivity between the PCC and other DMN areas. This study, in conjunction with previous research, might help to elucidate that the anomalous connectivity patterns could be the brain circuit mechanisms underlying the pathophysiology of schizophrenia.

5. Limitations

Limitations should be considered. First, the sample size of this study was relatively small, which could limit the generalizability of prediction models (Jollans et al., 2019). Here, we only used rs-fMRI in the current study. Larger sample size with additional neuroimaging modalities, such as structural neuroimaging and diffusion tensor imaging, could be added to improve classification performance in this context. Second, using a seed-based approach, FC patterns were based on the predefined seed region, the addition of an independent component analysis approach would be advantageous in future studies. Third, the potential comorbidities (metabolic syndrome, obsessional traits, and disturbances of circadian rhythm) on brain connectivity in participants with schizophrenia requires further investigations. Fourth, we were unable to account for the possible effect of pharmacological treatment even in a limited numbers of affected participants. Fifth, cardio-respiratory related physiological noise during scanning were not removed in this study.

6. Conclusion

In the current study, we identified the differential PCC-based functional connectivity which greatly contributed to distinguishing patients with FES from HC individuals. Using the PCC-based regional-wise connectivity, in combination with machine learning algorithm, robustness was established with replication across the independent dataset.

Findings of the current study demonstrated that the proposed method not only achieved a promising classification performance for distinguishing schizophrenia patients from HC, but also identified discriminative brain pattern of predominant hypoconnectivity between the PCC and other DMN regions that were likely significant in relation to the neuronal underpinnings of pathophysiology in schizophrenia.

Role of the funding source

This work was funded by the Key Program of National Natural Science Foundation of China (T.L., grant number 81630030 & 81130024); the National Natural Science Foundation of China / the Research Grants Council (RGC) of Hong Kong Joint Research Scheme (T.L., grant number 81461168029); the National Key Technology R & D Program of China (T.L., grant number 2016YFC0904300); the 1.3.5 Project for Disciplines of Excellence, West China Hospital, Sichuan University (to T.L. and X.H. M.); the National Natural Science Foundation of China (S.L., grant number 81801326; W.D., grant number 81571320); the Sichuan Provincial S&T Projects (Q.W., grant number 2015JY0173). This research received no specific grant from any funding agency, commercial or not-for-profit sectors.

Contributors

Authors TL, WD and XM designed the study and wrote the protocol. Authors SL, WD, QW and CZ managed the literature searches and analyses. ML, YM and WG had interview with participants. HY, XL and LZ gathered data. Authors SL undertook the statistical analysis with some help from XK and AG, and author SL wrote the first draft of the manuscript. Authors AG, TL and XL were involved in the revision and completion of the work. All authors contributed to and have approved the final manuscript.

Declaration of competing interest

None.

Acknowledgments

All subjects participating in the study are most warmly thanked.

Appendix A. Supplementary data

Supplementary data to this article can be found online at <https://doi.org/10.1016/j.schres.2020.03.022>.

References

- Andrews-Hanna, J.R., Snyder, A.Z., Vincent, J.L., Lustig, C., Head, D., Raichle, M.E., Buckner, R.L., 2007. Disruption of large-scale brain systems in advanced aging. *Neuron* 56 (5), 924–935.
- Bazin, P.-L., Shiee, N., Ellingsen, L.M., Prince, J.L., Pham, D.L., 2011. Digital topology in brain image segmentation and registration. In: El-Baz, A.S., Acharya, U.R., Mirmehdi, M., Suri, J.S. (Eds.), *Multi Modality State-of-the-Art Medical Image Segmentation and Registration Methodologies*. 1. Springer US, Boston, MA, pp. 339–375.
- Bluhm, R.L., Miller, J., Lanius, R.A., Osuch, E.A., Boksman, K., Neufeld, R.W., Theberge, J., Schaefer, B., Williamson, P., 2007. Spontaneous low-frequency fluctuations in the BOLD signal in schizophrenic patients: anomalies in the default network. *Schizophr. Bull.* 33 (4), 1004–1012.
- Buckner, R.L., Andrews-Hanna, J.R., Schacter, D.L., 2008. The brain's default network: anatomy, function, and relevance to disease. *Ann. N. Y. Acad. Sci.* 1124, 1–38.
- Chekroud, A.M., Zotti, R.J., Shehzad, Z., Gueorguieva, R., Johnson, M.K., Trivedi, M.H., Cannon, T.D., Krystal, J.H., Corlett, P.R., 2016. Cross-trial prediction of treatment outcome in depression: a machine learning approach. *Lancet Psychiatry* 3 (3), 243–250.
- Cheng, W., Palaniyappan, L., Li, M., Kendrick, K.M., Zhang, J., Luo, Q., Liu, Z., Yu, R., Deng, W., Wang, Q., Ma, X., Guo, W., Francis, S., Liddle, P., Mayer, A.R., Schumann, G., Li, T., Feng, J., 2015. Voxel-based, brain-wide association study of aberrant functional connectivity in schizophrenia implicates thalamocortical circuitry. *NPJ Schizophr.* 1, 15016.
- Ciric, R., Wolf, D.H., Power, J.D., Roalf, D.R., Baum, G.L., Ruparel, K., Shinohara, R.T., Elliott, M.A., Eickhoff, S.B., Davatzikos, C., Gur, R.C., Gur, R.E., Bassett, D.S., Satterthwaite, T.D., 2017. Benchmarking of participant-level confound regression strategies for the control of motion artifact in studies of functional connectivity. *NeuroImage* 154, 174–187.
- Du, Y., Pearson, G.D., Yu, Q., He, H., Lin, D., Sui, J., Wu, L., Calhoun, V.D., 2016. Interaction among subsystems within default mode network diminished in schizophrenia patients: a dynamic connectivity approach. *Schizophr. Res.* 170 (1), 55–65.
- Ebisch, S.J.H., Gallese, V., Salone, A., Martinotti, G., di Iorio, G., Mantini, D., Perrucci, M.G., Romani, G.L., Di Giannantonio, M., Northoff, G., 2018. Disrupted relationship between “resting state” connectivity and task-evoked activity during social perception in schizophrenia. *Schizophr. Res.* 193, 370–376.
- Fransson, P., Marrelec, G., 2008. The precuneus/posterior cingulate cortex plays a pivotal role in the default mode network: evidence from a partial correlation network analysis. *NeuroImage* 42 (3), 1178–1184.
- Friedman, J.H., 2001. Greedy function approximation: a gradient boosting machine. *Ann. Stat.* 29 (5), 1189–1232.
- Gao, X., Zhang, W., Yao, L., Xiao, Y., Liu, L., Liu, J., Li, S., Tao, B., Shah, C., Gong, Q., Sweeney, J.A., Lui, S., 2018. Association between structural and functional brain alterations in drug-free patients with schizophrenia: a multimodal meta-analysis. *J. Psychiatry Neurosci.* 43 (2), 131–142.
- Garrity, A.G., Pearlson, G.D., McKiernan, K., Lloyd, D., Kiehl, K.A., Calhoun, V.D., 2007. Aberrant “default mode” functional connectivity in schizophrenia. *Am. J. Psychiatry* 164 (3), 450–457.
- Gotts, S.J., Saad, Z.S., Jo, H.J., Wallace, G.L., Cox, R.W., Martin, A., 2013. The perils of global signal regression for group comparisons: a case study of Autism Spectrum Disorders. *Front. Hum. Neurosci.* 7, 356.
- Greicius, M.D., Krasnow, B., Reiss, A.L., Menon, V., 2003. Functional connectivity in the resting brain: a network analysis of the default mode hypothesis. *Proc. Natl. Acad. Sci. U. S. A.* 100 (1), 253–258.
- Haznedar, M.M., Buchsbaum, M.S., Hazlett, E.A., Shihabuddin, L., New, A., Siever, L.J., 2004. Cingulate gyrus volume and metabolism in the schizophrenia spectrum. *Schizophr. Res.* 71 (2–3), 249–262.
- Jenkinson, M., Bannister, P., Brady, M., Smith, S., 2002. Improved optimization for the robust and accurate linear registration and motion correction of brain images. *NeuroImage* 17 (2), 825–841.
- Jollans, L., Boyle, R., Artiges, E., Banaschewski, T., Desrivieres, S., Grigis, A., Martinot, J.L., Paus, T., Smolka, M.N., Walter, H., Schumann, G., Garavan, H., Whelan, R., 2019. Quantifying performance of machine learning methods for neuroimaging data. *NeuroImage* 199, 351–365.
- Lee, H., Lee, D.K., Park, K., Kim, C.E., Ryu, S., 2019. Default mode network connectivity is associated with long-term clinical outcome in patients with schizophrenia. *NeuroImage Clin.* 22, 101805.
- Leech, R., Sharp, D.J., 2014. The role of the posterior cingulate cortex in cognition and disease. *Brain* 137 (Pt 1), 12–32.
- Li, J., Sun, Y., Huang, Y., Bezerianos, A., Yu, R., 2019. Machine learning technique reveals intrinsic characteristics of schizophrenia: an alternative method. *Brain Imaging Behav.* 13 (5), 1386–1396.
- Liang, S., Li, Y., Zhang, Z., Kong, X., Wang, Q., Deng, W., Li, X., Zhao, L., Li, M., Meng, Y., Huang, F., Ma, X., Li, X.M., Greenshaw, A.J., Shao, J., Li, T., 2019. Classification of first-episode schizophrenia using multimodal brain features: a combined structural and diffusion imaging study. *Schizophr. Bull.* 45 (3), 591–599.
- Lin, P., Yang, Y., Jovicich, J., De Pisapia, N., Wang, X., Zuo, C.S., Levitt, J.J., 2016. Static and dynamic posterior cingulate cortex nodal topology of default mode network predicts attention task performance. *Brain Imaging Behav.* 10 (1), 212–225.
- Meng, X., Jiang, R., Lin, D., Bustillo, J., Jones, T., Chen, J., Yu, Q., Du, Y., Zhang, Y., Jiang, T., Sui, J., Calhoun, V.D., 2016. Predicting individualized clinical measures by a generalized prediction framework and multimodal fusion of MRI data. *NeuroImage* 145 (Pt B), 218–229.
- Mikolas, P., Melicher, T., Koch, A., Matejka, M., Slovakova, A., Bakstein, E., Hajek, T., Spaniel, F., 2016. Connectivity of the anterior insula differentiates participants with first-episode schizophrenia spectrum disorders from controls: a machine-learning study. *Psychol. Med.* 46 (13), 2695–2704.
- Mitelman, S.A., Shihabuddin, L., Brickman, A.M., Hazlett, E.A., Buchsbaum, M.S., 2005. Volume of the cingulate and outcome in schizophrenia. *Schizophr. Res.* 72 (2–3), 91–108.
- Natekin, A., Knoll, A., 2013. Gradient boosting machines, a tutorial. *Front. Neurobot.* 7, 21.
- Newell, K.A., Deng, C., Huang, X.F., 2006. Increased cannabinoid receptor density in the posterior cingulate cortex in schizophrenia. *Exp. Brain Res.* 172 (4), 556–560.
- Northoff, G., Richter, A., Bermpohl, F., Grimm, S., Martin, E., Marcar, V.L., Wahl, C., Hell, D., Boeker, H., 2005. NMDA hypofunction in the posterior cingulate as a model for schizophrenia: an exploratory ketamine administration study in fMRI. *Schizophr. Res.* 72 (2–3), 235–248.
- Pedregosa, F., Varoquaux, G., Gramfort, A., Michel, V., Thirion, B., Grisel, O., Blondel, M., Prettenhofer, P., Weiss, R., Dubourg, V., 2011. Scikit-learn: machine learning in python. *J. Mach. Learn. Res.* 12 (Oct), 2825–2830.
- Power, J.D., Barnes, K.A., Snyder, A.Z., Schlaggar, B.L., Petersen, S.E., 2012. Spurious but systematic correlations in functional connectivity MRI networks arise from subject motion. *NeuroImage* 59 (3), 2142–2154.
- Raichle, M.E., MacLeod, A.M., Snyder, A.Z., Powers, W.J., Gusnard, D.A., Shulman, G.L., 2001. A default mode of brain function. *Proc. Natl. Acad. Sci. U. S. A.* 98 (2), 676–682.
- Rotarska-Jagiela, A., van de Ven, V., Oertel-Knochel, V., Uhlhaas, P.J., Vogeley, K., Linden, D.E., 2010. Resting-state functional network correlates of psychotic symptoms in schizophrenia. *Schizophr. Res.* 117 (1), 21–30.
- Samartzis, L., Dima, D., Fusar-Poli, P., Kyriakopoulos, M., 2014. White matter alterations in early stages of schizophrenia: a systematic review of diffusion tensor imaging studies. *J. Neuroimaging* 24 (2), 101–110.
- Smith, S.M., Jenkinson, M., Woolrich, M.W., Beckmann, C.F., Behrens, T.E., Johansen-Berg, H., Bannister, P.R., De Luca, M., Drobnjak, I., Flitney, D.E., Niaz, R.K., Saunders, J., Vickers, J., Zhang, Y., De Stefano, N., Brady, J.M., Matthews, P.M., 2004. Advances in functional and structural MR image analysis and implementation as FSL. *NeuroImage* 23 (Suppl. 1), S208–S219.
- Spreng, R.N., Mar, R.A., Kim, A.S., 2009. The common neural basis of autobiographical memory, prospection, navigation, theory of mind, and the default mode: a quantitative meta-analysis. *J. Cogn. Neurosci.* 21 (3), 489–510.
- Van Dijk, K.R., Hedden, T., Venkataraman, A., Evans, K.C., Lazar, S.W., Buckner, R.L., 2010. Intrinsic functional connectivity as a tool for human connectomics: theory, properties, and optimization. *J. Neurophysiol.* 103 (1), 297–321.
- Venkataraman, A., Whitford, T.J., Westin, C.F., Golland, P., Kubicki, M., 2012. Whole brain resting state functional connectivity abnormalities in schizophrenia. *Schizophr. Res.* 139 (1–3), 7–12.
- Whitfield-Gabrieli, S., Thermenos, H.W., Milanovic, S., Tsuang, M.T., Faraone, S.V., McCarley, R.W., Shenton, M.E., Green, A.J., Nieto-Castanon, A., LaViolette, P., Wojcik, J., Gabrieli, J.D., Seidman, L.J., 2009. Hyperactivity and hyperconnectivity of the default

- network in schizophrenia and in first-degree relatives of persons with schizophrenia. *Proc. Natl. Acad. Sci. U. S. A.* 106 (4), 1279–1284.
- Wong, D.F., Kuwabara, H., Horti, A.G., Raymond, V., Brasic, J., Guevara, M., Ye, W., Dannals, R.F., Ravert, H.T., Nandi, A., Rahmim, A., Ming, J.E., Grachev, I., Roy, C., Cascella, N., 2010. Quantification of cerebral cannabinoid receptors subtype 1 (CB1) in healthy subjects and schizophrenia by the novel PET radioligand [¹¹C]OMAR. *NeuroImage* 52 (4), 1505–1513.
- Xia, M., Wang, J., He, Y., 2013. BrainNet Viewer: a network visualization tool for human brain connectomics. *PLoS One* 8 (7), e68910.
- Yang, G.J., Murray, J.D., Repovs, G., Cole, M.W., Savic, A., Glasser, M.F., Pittenger, C., Krystal, J.H., Wang, X.J., Pearlson, G.D., Glahn, D.C., Anticevic, A., 2014. Altered global brain signal in schizophrenia. *Proc. Natl. Acad. Sci. U. S. A.* 111 (20), 7438–7443.
- Yu, Q., Allen, E.A., Sui, J., Arbabshirani, M.R., Pearlson, G., Calhoun, V.D., 2012. Brain connectivity networks in schizophrenia underlying resting state functional magnetic resonance imaging. *Curr. Top. Med. Chem.* 12 (21), 2415–2425.
- Zhang, Z., Yan, T., Wang, Y., Zhang, Q., Zhao, W., Chen, X., Zhai, J., Chen, M., Du, B., Deng, X., Ji, F., Xiang, Y., Wu, H., Song, J., Dong, Q., Chen, C., Li, J., 2018. Polymorphism in schizophrenia risk gene MIR137 is associated with the posterior cingulate Cortex's activation and functional and structural connectivity in healthy controls. *Neuroimage Clin.* 19, 160–166.
- Zhou, Y., Shu, N., Liu, Y., Song, M., Hao, Y., Liu, H., Yu, C., Liu, Z., Jiang, T., 2008. Altered resting-state functional connectivity and anatomical connectivity of hippocampus in schizophrenia. *Schizophr. Res.* 100 (1–3), 120–132.